

Understanding the Protected Nodes and Collapse of the Fermi Arcs in Underdoped Cuprate Superconductors

Qijin Chen and K. Levin

James Franck Institute and Department of Physics, University of Chicago, Chicago, Illinois 60637

(Dated: October 20, 2019)

We show how recent angle resolved photoemission measurements on the cuprates, demonstrating the collapse of the Fermi arcs below T_c , reveal a very natural phenomenological description of the complex superfluid phase. Importantly, this phenomenology is consistent with a previously presented microscopic theory. The collapse of the arcs into well defined nodes is associated with the emergence of superconducting order. Comparison of this theory with experiment shows good semi-quantitative agreement and serves to reconcile other paradoxical behavior in the superconducting phase with these unusual photoemission data.

PACS numbers: PACS numbers: 74.20.-z, 74.20.Fg, 74.25.Bt, 74.25.Fy

arXiv:0712.1253

In the past most of the interest in lower T_c cuprate superconductors has focused on the exotic, non-Fermi liquid normal phase. In a recent paper by Kanigel et al,¹ angle resolved photoemission experiments on several underdoped samples of $\text{Bi}_2\text{Sr}_2\text{CaCu}_2\text{O}_8$ (Bi2212) were used to establish key features of the superconducting phase. In particular, it was reported¹ that (i) the photo-emission-measured excitation gap, $\Delta(\mathbf{k}, T)$ is roughly constant in temperature from $T = 0$ to above T_c . (ii) Below T_c , $\Delta(\mathbf{k})$ displays the d -wave point nodes which broaden into Fermi arcs above T_c , with the change occurring within the width of the resistive transition at T_c . (iii) It is claimed² that the energy scale of the excitation gap is T^* , or the pseudogap^{3,4} onset temperature, and that the Fermi arc length scales with T/T^* above T_c . From (i) it is inferred that (iv) “the energy gap is *not* directly related to the superconducting order parameter”.

These latest experiments have underlined the fact that the *superfluid phase* is itself very complex in the presence of a normal state gap or “pseudogap”.^{3,4} Here we use these important photoemission observations to reveal a very natural phenomenological description of the superfluid phase. We then review a microscopic model consistent with this phenomenology which has been demonstrated⁴ to be compatible with a variety of other experiments. This microscopic (or phenomenological) approach yields good semi-quantitative agreement with a large number of different representations of these recent photoemission data.

Our microscopic scheme is based on a BCS–Bose-Einstein condensation (BEC) crossover scenario^{4,5,6} and is distinct from the phase fluctuation scenario.^{7,8} It has been argued⁹ to be appropriate to the cuprates because of their very short coherence length. We emphasize the generic features of our framework. One assumes that there are attractive interactions which lead to pairing and that this pairing gives rise to a gap in the fermionic spectrum both above and below T_c , and the gap hence should be viewed as distinct from superconducting order. The existence of a pseudogap above T_c reveals that noncondensed pairs can contribute to a gap, as do condensed pairs. Therefore, below T_c the gap contains two contributions, that from the condensed pairs Δ_{sc} , and that from the noncondensed pairs, Δ_{pg} . Since the pair density is associated with

the square of the gap, these contributions add in quadrature to yield for the total excitation gap squared, Δ^2

$$\Delta^2 = \Delta_{sc}^2 + \Delta_{pg}^2. \quad (1)$$

The same equation is deduced from points (i) and (iv) above. In order for the excitation gap $\Delta(\mathbf{k}, T)$ to be roughly a constant in T and evolve continuously from above to below T_c , there must be another component to the excitation gap below T_c , which compensates for the T dependence in $\Delta_{sc}(T)$. The simplest approach is to think of this term (i.e., $\Delta_{pg}^2(T)$) as a “fluctuation” contribution of the form $\langle \Delta^2 \rangle - \langle \Delta \rangle^2$.

The normal state analysis of ARPES experiments has already made substantial use^{10,11,12} of a broadened BCS form¹³ for the fermion self energy

$$\Sigma_{pg}(\mathbf{k}, \omega) = \frac{\Delta_{\mathbf{k}, pg}^2}{\omega + \epsilon_{\mathbf{k}} + i\gamma} - i\Sigma_0 \quad (2)$$

where the broadening $\gamma \neq 0$ and “incoherent” background contribution Σ_0 reflect that noncondensed pairs do not lead to *true* off-diagonal long-range order. We adopt a tight binding model for the band dispersion $\epsilon_{\mathbf{k}}$. The detailed band structure, is of no importance in our calculations which address ARPES data points along the Fermi surface $\epsilon_{\mathbf{k}} = 0$. Here the pseudogap $\Delta_{\mathbf{k}, pg} = \Delta_{pg}\varphi_{\mathbf{k}}$, and we introduce $\varphi_{\mathbf{k}} = \cos(2\phi)$, to reflect the d -wave \mathbf{k} dependence. A key result of this paper is that in the superfluid phase there should be an additional component of the self energy arising from the condensate, Σ_{sc} so that

$$\Sigma(\mathbf{k}, \omega) = \Sigma_{pg}(\mathbf{k}, \omega) + \Sigma_{sc}(\mathbf{k}, \omega) \quad (3)$$

$$\Sigma_{sc}(\mathbf{k}, \omega) = \frac{\Delta_{\mathbf{k}, sc}^2}{\omega + \epsilon_{\mathbf{k}}}, \quad (4)$$

with $\Delta_{\mathbf{k}, sc} = \Delta_{sc}\varphi_{\mathbf{k}}$. Since Σ_{sc} is associated with long-lived condensed Cooper pairs rather than finite-lifetime incoherent pairs, it is of the same form as Σ_{pg} but without the broadening. With this self energy in the Green’s functions, the resulting spectral function, $A(\mathbf{k}, \omega) = -2 \text{Im} G(\mathbf{k}, \omega + i0)$ can be readily determined. One can see that the spectral function at all \mathbf{k} contains a zero at $\omega = -\epsilon_{\mathbf{k}}$ below T_c , whereas it has no zero

above T_c . This dramatic effect of superconducting coherence will be reflected in the disappearance of Fermi arcs below T_c .

Since Δ_{pg} represents a contribution from thermal bosonic fluctuations, it should vanish in the ground state and roughly be of the general form

$$\Delta_{pg}^2(T) = (T/T_c)^\nu \Delta^2(T_c), \quad T \leq T_c. \quad (5)$$

Using this equation one can determine T_c as the the lowest temperature at which $\Delta_{sc} = 0$. The exponent ν in general varies between 3 and 3/2, which corresponds to linear and quadratic pair dispersion, respectively. What is important is not the value of ν , but that at T_c the order parameter vanishes, and the term Δ_{pg} accounts for the entire excitation gap $\Delta(T_c)$.

Because $\Delta(T) \approx \Delta(T_c)$, in the underdoped regime it seems difficult to understand how the superfluid density n_s vanishes at T_c when the number of fermionic excitations ($\propto T/\Delta$) is smaller than the total fermion number for all $T \leq T_c$. The phase fluctuation scenario addresses this question by invoking bosonic excitations, but generally ignores the fermionic degrees of freedom.⁷ Here we argue that we have enough evidence associated with long lived d -wave, Bogoliubov quasiparticles^{3,4,14,15} and other experiments^{16,17} below T_c , to suggest that we not entirely abandon the BCS framework. We are led to postulate a simple BCS-like expression for the superfluid density¹⁸

$$\left(\frac{n_s}{m}\right) = \left[1 - \frac{\Delta_{pg}^2(T)}{\Delta^2(T)}\right] \left(\frac{n_s^{BCS}(T, \Delta)}{m}\right), \quad (6)$$

where the quantity (n_s^{BCS}/m) represents the conventional BCS superfluid density with T -independent gap. The second term above in the square brackets represents the contribution from bosonic fluctuations.

The observation of a BCS-like scaling law,^{16,17} $T^* \approx 2\Delta(0)/4.3$, suggests that, for all $T < T^*$, we attribute a BCS form to the gap $\Delta(T)$, rather than to the order parameter $\Delta_{sc}(T)$

$$1 + U \sum_{\mathbf{k}} \frac{1 - 2f(E_{\mathbf{k}})}{2E_{\mathbf{k}}} \varphi_{\mathbf{k}}^2 = 0, \quad (7)$$

Here $E_{\mathbf{k}} = \sqrt{\epsilon_{\mathbf{k}}^2 + \Delta_{\mathbf{k}}^2}$, with $\Delta_{\mathbf{k}} = \Delta \varphi_{\mathbf{k}}$; $U < 0$ is the pairing interaction strength,¹⁸ and $f(x)$ is the Fermi function. The ratio $\Delta(T)/\Delta(0)$ as a function of T/T^* is then given by a nearly universal curve independent of the doping concentration, x . In the underdoped regime, $\Delta(T_c)$ is large so that Eq. (7) is consistent with a very high $T^* \gg T_c$ and a roughly constant gap within the superfluid phase.

We briefly present a T -matrix approach from which Eqs. (1) - (7) were previously derived, noting that more details can be found elsewhere.⁴ We start by observing that the BCS-like constraint in Eq. (7) can be interpreted as equivalent to the BEC condition that the noncondensed pairs have zero chemical potential

$$\mu_{pair} = 0 \quad (8)$$

at and below T_c . This determines the form of the noncondensed pair propagator $t_{pg}(Q) = U/[1 + U\chi(Q)]$ such that

$t_{pg}(0) = \infty$ at $T \leq T_c$, where $\chi(Q) = \sum_K G_0(Q - K)G(K)\varphi_{\mathbf{k}-\mathbf{q}/2}^2$, is the pair susceptibility. Here G and G_0 are the full and bare Green's functions, respectively. To make direct association with Eq. (7), we drop the γ and Σ_0 term (which are more important above than below T_c) in Eq. (2) and arrive at $\Sigma(\mathbf{k}, \omega) \approx \Delta_{\mathbf{k}}^2/(\omega + \epsilon_{\mathbf{k}})$ for $T \leq T_c$. This reasonable approximation can be used to determine the form for G , and establish an equivalence between Eqs. (7) and (8).

To establish the validity of Eqs. (2) and (4), we note that there are two contributions to the full T -matrix $t = t_{pg} + t_{sc}$ where the condensate contribution $t_{sc}(Q) = -\frac{\Delta_{sc}^2}{T}\delta(Q)$. Similarly, we have for the fermion self energy $\Sigma(K) = \Sigma_{sc}(K) + \Sigma_{pg}(K) = \sum_Q t(Q)G_0(Q - K)\varphi_{\mathbf{k}-\mathbf{q}/2}^2$, from which Eq. (4) follows at once. A vanishing chemical potential means that $t_{pg}(Q)$ diverges at $Q = 0$ when $T \leq T_c$. Thus, in the superfluid phase only, we approximate^{13,19} $\Sigma_{pg}(K)$ to yield $\Sigma_{pg}(K) \approx -G_0(-K)\Delta_{\mathbf{k},pg}^2$, where $\Delta_{pg}^2 \equiv -\sum_{Q \neq 0} t_{pg}(Q)$. We thus may write $\Sigma_{pg}(\mathbf{k}, \omega) = \Delta_{\mathbf{k},pg}^2(T)/(\omega + \epsilon_{\mathbf{k}}) + \text{small corrections}$, where we accommodate the corrections¹³ with the broadening factor γ and additional term Σ_0 . This is necessary in order to address the *concrete* fermion spectral function. In this way, Eq. (2) then follows. Finally, at small four-vector $Q \equiv (\Omega, \mathbf{q})$, we expand the inverse of t_{pg} , after analytical continuation, to obtain a simple quadratic dispersion⁴ for the pairs $\Omega_{\mathbf{q}} \approx q^2/(2M^*)$, implying $\nu = 3/2$.

To emphasize the simplicity and physical accessibility of this approach which builds on the ground state of the BCS-Leggett wavefunction,⁵ we proceed within the phenomenological scheme. For a given doping concentration, $\Delta(0)$, $\Delta(T_c)$, T_c and T^* are presumed known, one can then determine $\Delta(T)$ based on the universal curve for $\Delta(T)/\Delta(0)$ versus T/T^* . Finally, one determines Δ_{sc} and Δ_{pg} below T_c using Eqs. (1) and (5). In our numerics, we choose Σ_0 and γ via a rough fit to ARPES data near T_c ($\approx 95K$) and near optimal doping. Since Σ_0 is primarily governed by the particle-hole channel,¹⁰ we take it to be independent of doping and T , and given by $\Sigma_0 = 22.5$ meV. The broadening parameter γ depends primarily on temperature. We take $\gamma = 22.5$ meV at 95 K, and $\gamma = \gamma(T_c)(T/T_c)$ above T_c and $\gamma = \gamma(T_c)(T/T_c)^3$ below T_c , as used earlier.¹⁰ Throughout $\phi = 0$ and $\pi/4 = 45^\circ$ denote the anti-nodal and nodal directions, respectively. In order to compare with ARPES data, we convolve the spectral function with a Gaussian instrumental broadening curve choosing standard deviation $\sigma = 3$ meV, given by the ideal ARPES resolution. To illustrate the simple physics, we do not attempt to do detailed curve fitting. Nevertheless, these parameters optimize the overall agreement with experiment.

In the inset to Fig. 1(b) we plot the various gap parameters Δ_{sc} , Δ and Δ_{pg} as a function of temperature below T_c and slightly above, for a typical underdoped system. Here for definiteness we have chosen $\nu = 3/2$ in Eq. (5). It can be seen that, as T is lowered below T_c , the total excitation gap Δ is essentially a constant while Δ_{sc} increases from 0 at T_c to reach the full gap value at $T = 0$. By contrast, Δ_{pg} monotonically decreases to 0.

In Figs. 1(a) and 1(b), we plot the spectral function $A(\omega)$

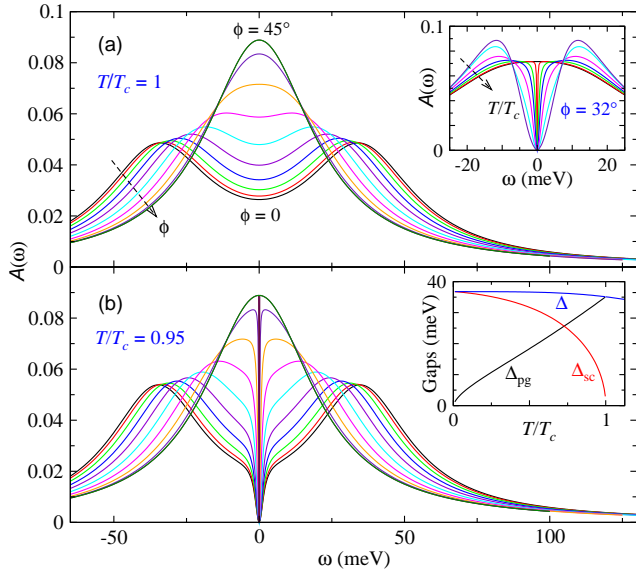


Figure 1: (color online) Spectral function $A(\omega)$ for $x = 0.125$ at (a) $T = T_c$ and (b) $0.95T_c$ at different angles ϕ along the Fermi surface of a cuprate superconductor, where ϕ increases by 4.5° from 0 to 45° along the direction of the arrow. The upper inset shows the temperature dependence of $A(\omega)$ at $\phi = 32^\circ$ near the node, with $T/T_c = 1, 0.99, 0.95, 0.9, 0.8, 0.6$ and 0.3 in the direction of the arrow. Shown in the lower inset are the gaps vs T below T_c . The effects of phase coherence are more pronounced in the nodal region of the Fermi surface, where the gap is small.

for $\epsilon_{\mathbf{k}} = 0$ (on the Fermi surface) at and slightly below T_c , respectively, and for different angles. To illustrate the physics, here we do not include the ARPES instrumental broadening. Just below T_c , the sharp dip at $\omega = 0$ is associated with the onset of a very small condensate, which nevertheless leads to a depletion of the spectral weight at the Fermi level. The coherence associated with the order parameter is better illustrated near the nodal region where a gap, absent at T_c , appears as T decreases, as shown for $\phi = 32^\circ$ in the upper inset. A closer inspection of the shape of $A(\omega)$ in Fig. 1(b) suggests that $A(\omega)$ cannot be described by a simple broadened BCS spectral function.

Figure 2 presents a plot of the spectroscopic gap for an underdoped cuprate with $x = 0.125$ as a function of angle and for various temperatures below (dashed curves) and above T_c (solid curves). Here the gap is given by half the peak-to-peak distance in the spectral function. For $T < T_c$, since the gap is roughly T independent, the various curves tend to coalesce. Above T_c , the extended range of zero gap value around $\phi = 45^\circ$ gives rise to the Fermi arcs.^{11,12} This is due to the presence of γ . The rapid deviation of the (red dashed) $T = 0.99T_c$ curve from the (black solid) $T = T_c$ curve indicates a collapse of the Fermi arc, leading to the protected nodes below T_c , reflecting the emergence of superconducting order below T_c . This figure should be compared with Fig. 2 of Ref. 1.

In Fig. 3 we plot the relative loss of spectral weight $L(\phi) = 1 - I(0)/I(\Delta_\phi)$, defined following Ref. 1, at the anti-node

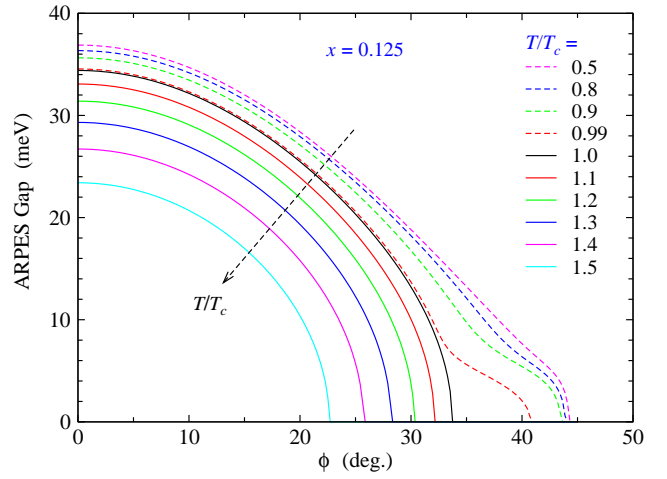


Figure 2: (color online) Spectral gap as measured in ARPES as a function of angle ϕ along the Fermi surface of an underdoped cuprate superconductor of doping $x = 0.125$, at different T/T_c between 0.5 and 1.5 . The spectral function has been broadened with a small ARPES instrumental resolution of 3 meV. A Fermi arc appears as the extended range of zero gap value. The fast departure of the $T = 0.99T_c$ curve from the $T = T_c$ curve indicates a collapse of the Fermi arc.

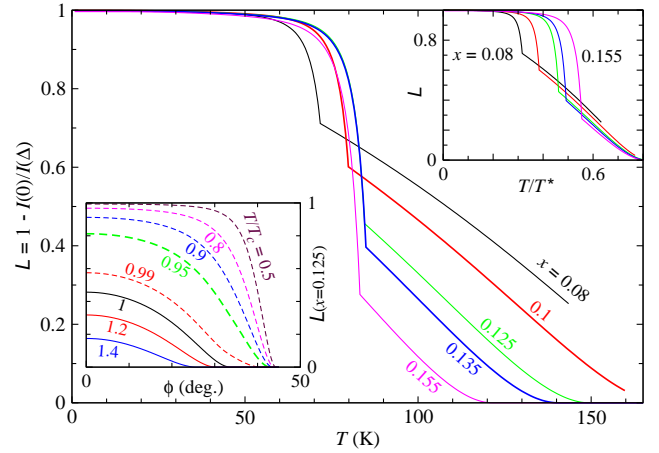


Figure 3: (color online) Loss of zero energy spectral weight as a function of temperature at the antinode, for different hole concentrations. Upper right inset shows rescaled T dependence, while lower left inset indicates ϕ dependence for various T .

$\phi = 0$ as a function of T for different doping concentrations, where $I(\omega) \equiv A(\omega)$. The lower left inset presents plots of $L(\phi)$ as a function of ϕ for various temperatures while the upper right inset illustrate the anti-node behavior $L(\phi = 0)$ as a function of T/T^* . Here (and throughout) T^* is estimated from Eq. (7). It can be seen from the upper inset that there is considerable universality above T_c as a function of T/T^* , which provides a prediction for a future representation of ARPES data. Here $x = 0.08$ and $x = 0.135$ roughly correspond, respectively, to the 67K and 80K samples of Ref. 1. The comparison of the black and blue curves with the upper panel of Fig. 4 of Ref. 1 shows good agreement. Above T_c the

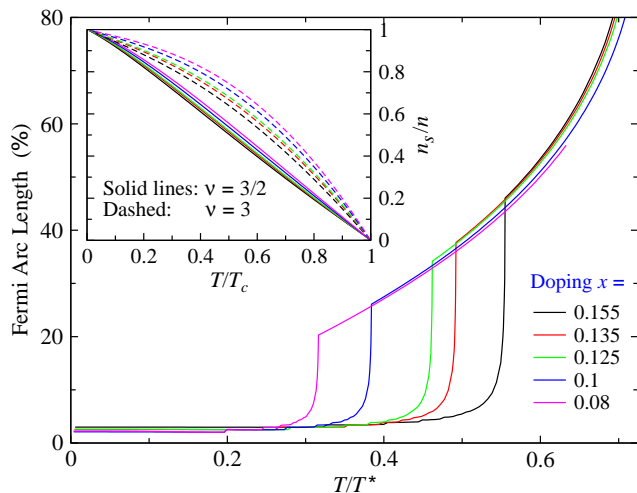


Figure 4: (color online) Fermi arc length as a function of T/T^* for different doping concentrations from optimal to underdoping for a cuprate superconductor. Fermi arc length is typically finite above T_c and drops to zero once phase coherence is established below T_c . The normal state portions of the curves is close to universal, in agreement with Ref. 2. Plotted in the inset is the quasi-universal behavior of n_s/n as a function of T/T_c for various x and for different power law exponents $\nu = 3/2$ (solid) and 3 (dashed lines). The inset shares the color coding with the main figure.

dependence is linear in T reflecting a linear T dependence in γ . As the temperature decreases, the abrupt jump across T_c reflects the onset of phase coherence, as in Fig. 2.

Finally, Fig. 4 shows the sharp collapse of the Fermi arcs from above to below T_c ; we plot the percentage of the arc length as a function of T/T^* and for different hole concentrations in the optimal to underdoped regimes. The small nonva-

nishing arc length reflects the finite ARPES resolution. As a consequence of the Fermi arc collapse below T_c , the nodes are “protected”. In addition, there is a clear universality seen in the normal state, as has been discussed in Ref. 2. Our results are in good agreement with the central features observed experimentally, shown in Fig. 4 of Refs. 1 and 2. Unlike Ref. 1, however, our curves are not strictly straight lines, reflecting the nonlinearity of the gap as a function of $\phi - \pi/4$; this seems to be consistent with Fig. 4 of Ref. 2.

The inset of Fig. 4 shows the behavior of the superfluid density as a function of temperature for different values of ν in Eq. (5) corresponding to $\nu = 3/2$ (solid) and 3 (dashed lines) and for different hole concentrations. Both sets of curves show a fair degree of “universality”, as has been observed experimentally.^{3,4} This suggests that the detailed power law in Eq. (5) is not essential to the physics.

The microscopic approach⁴ considered here is associated with stronger-than-BCS attractive interactions which lead to small pair size. A major consequence of this theory (as well as the equivalent phenomenology which ARPES experiments lead us to infer), is that *pseudogap effects persist below T_c in the form of noncondensed pair excitations of the condensate*. Importantly, this leads to two contributions to the self energy below T_c [see Eq. (4)] which enter into the spectral function. As a result we find that the collapse of the Fermi arcs is not to be associated with an abrupt disappearance of the inverse pair lifetime γ , appearing in Σ_{pg} , but rather it reflects the gradual emergence of the condensate, appearing in Σ_{sc} , to which the finite momentum pairs are continuously converted as T decreases. Recognition of the complexity of the superfluid phase represents a new direction for the field.

This work was supported by NSF Grants No. PHY-0555325 and No. MRSEC DMR-0213745.

¹ A. Kanigel, U. Chatterjee, M. Randeria, M. R. Norman, S. Souma, M. Shi, Z. Z. Li, H. Raffy, and J. C. Campuzano, Phys. Rev. Lett. **99**, 157001 (2007).
² A. Kanigel et al., Nature Physics **2**, 447 (2006).
³ P. Lee, N. Nagaosa, and X. G. Wen, Review of Modern Physics **78**, 17 (2006).
⁴ Q. J. Chen, J. Stajic, S. N. Tan, and K. Levin, Phys. Rep. **412**, 1 (2005); K. Levin and Q. J. Chen, e-print cond-mat/0610006.
⁵ A. J. Leggett, in *Modern Trends in the Theory of Condensed Matter* (Springer-Verlag, Berlin, 1980), pp. 13–27.
⁶ M. Randeria, in *Proceedings of the International School of Physics “Enrico Fermi” Course CXXXVI on High Temperature Superconductors*, edited by G. Iadonisi, J. R. Schrieffer, and M. L. Chialfalo (IOS, Amsterdam, 1998), p. 53.
⁷ V. J. Emery and S. A. Kivelson, Nature **374**, 434 (1995).
⁸ M. Franz, Z. Tesanovic, and O. Vafek, Phys. Rev. B **66**, 054535 (2002).
⁹ A. J. Leggett, Nature Physics **2**, 134 (2006).
¹⁰ Q. J. Chen, K. Levin, and I. Kosztin, Phys. Rev. B **63**, 184519 (2001).

¹¹ M. R. Norman, A. Kanigel, M. Randeria, U. Chatterjee, and J. C. Campuzano, Phys. Rev. B **76**, 174501 (2007).
¹² A. V. Chubukov, M. R. Norman, A. J. Millis, and E. Abrahams, Phys. Rev. B **76**, 180501(R) (2007).
¹³ J. Maly, B. Jankó, and K. Levin, Physica C **321**, 113 (1999).
¹⁴ J. C. Campuzano, M. R. Norman, and M. Randeria, in *Physics of Superconductors*, edited by K. H. Bennemann and J. B. Ketterson (Springer-Verlag, Berlin, 2004), vol. II, pp. 167–273.
¹⁵ R. Damascelli, Z. Hussain, and Z.-X. Shen, Rev. Mod. Phys. **75**, 473 (2003).
¹⁶ M. Oda, K. Hoya, R. Kubota, C. Manabe, N. Momono, T. Nakano, and M. Ido, Physica C **281**, 135 (1997).
¹⁷ M. Kugler, O. Fischer, C. Renner, S. Ono, and Y. Ando, Phys. Rev. Lett. **86**, 4911 (2001).
¹⁸ Q. J. Chen, I. Kosztin, B. Jankó, and K. Levin, Phys. Rev. Lett. **81**, 4708 (1998).
¹⁹ I. Kosztin, Q. J. Chen, B. Jankó, and K. Levin, Phys. Rev. B **58**, R5936 (1998).